Vol 18 No 3, March 2009
1674-1056/2009/18(03)/1077-08

Chinese Physics B

© 2009 Chin. Phys. Soc.
and IOP Publishing Ltd

Simultaneous all-solid-state multi-wavelength lasers—a promising pump source for generating highly coherent terahertz waves*

Liu Huan(刘 欢)[a)b)], Xu De-Gang(徐德刚)[a)†], and Yao Jian-Quan(姚建铨)[a)]

[a)] *Institute of Laser and Optoelectronics, College of Precision Instrument and Optoelectronics Engineering, Tianjin University, Tianjin* 300072, *China*

[b)] *Center for Photonics and Electronics, State Key Laboratory of Tribology, Department of Precision Instruments, Tsinghua University, Beijing* 100084, *China*

(Received 10 April 2008; revised manuscript received 31 July 2008)

A diode-end-pumped Nd:YAG dual-wavelength laser operating at 1319 and 1338 nm is demonstrated. The maximum average output power of the quasi-continuous wave linearly polarized dual-wavelength laser is obtained to be 2.1 W at a repetition rate of 50 kHz with an output power instability of less than 0.38% and beam quality factor M^2 of 1.45. Using the two lines, the highly coherent and narrow linewidth terahertz radiation of 3.23 THz can be generated in an organic 4-N, N-dimethylamino–methyl-stilbazolium tosylate (DAST) crystal. Meanwhile, the multi-wavelength red laser at 659.5, 664 and 669 nm is generated by frequency doubling and sum frequency processes in a lithium triborate (LBO) crystal. The average red laser output power is enhanced up to 1.625 W at a repetition rate of 15 kHz with an output power instability of better than 0.53% and beam quality factor M^2 of 6.05. Using the three lines, it is possible to generate the multi-wavelength THz radiation of 3.3, 3.43 and 6.73 THz in an appropriate difference frequency crystal.

Keywords: end-pumped Nd:YAG laser, dual-wavelength laser, acousto-optic Q-switch, terahertz wave

PACC: 4260B, 4260D, 4260F, 9580G

1. Introduction

Terahertz (THz) waves that exist between infrared and microwave are considered as one of the last unexplored frontiers in the electromagnetic spectrum.[1] With the recent developments of THz wave generation and detection techniques, THz wave technology has been applied to various scientific fields, such as medical imaging, chemical detection, broad band communication, astronomy, environmental inspection and safety inspection.[2] Generation of THz waves is one of key technologies in the THz field.[2−5] The methods of THz generation are divided into electronic method and photonic method. The nonlinear optical difference frequency method is one of the main methods to generate all-solid-state, low cost, compactable, room-temperature, and tunable THz wave radiation sources.[6−10] Recently, many researchers have devoted themselves to using the nonlinear optical difference frequency method to generate THz waves because of its compactness.[11−15] Of the key technologies of THz generation by using the nonlinear optical difference frequency method, developing novel difference frequency pumping sources which can simultaneously generate two or three close lasing lines with a high output power at room temperature is the most important. However, the reported difference frequency pumping sources are facing some problems, such as simultaneous operation of more than two separated lasers, bulkiness, and costliness.

As is well known, a rare-earth laser oscillates generally at one wavelength due to the differences in stimulated emission cross section (σ), fluorescence lifetime and fluorescence quantum efficiency. However, the rare-earth elements possess many energy levels and these energy levels of active ions can be split into a number of Stark sublevels due to the action of crystal field. Under special conditions, the laser can oscillate at more than one wavelength.[16−20] An Nd:YAG crystal is the most common laser gain medium be-

*Project supported by the National Basic Research Program of China (Grant No 2007CB310403) and the Tianjin Municipal Primary application and Frontier Technology Research Plan, China (Grant No 07JCYBJC06200).

†Corresponding author. E-mail: xudegang@tju.edu.cn

cause of its excellent physical and chemical properties and laser characteristics. Using Nd:YAG crystals, not only 1064, 1319 or 946 nm laser but also the dual-wavelength 1064 nm/946 nm, 1064 nm/1319 nm or 1319 nm/1338 nm laser has achieved a high output power.[21−23] 1319 nm and 1338 nm lasing lines are the two closely spaced transition lines with comparable values of σ, which can be used for highly coherent THz radiation by using the nonlinear optical difference frequency method.

In this paper, we demonstrate an efficient, all-solid-state diode-end-pumped Nd:YAG dual-wavelength laser operating at 1319 and 1338 nm. Using the two close lasing lines, the highly coherent and narrow linewidth THz radiation of 3.23 THz can be generated in a 1 mm thick DAST crystal. Meanwhile, the stable multi-wavelength red laser is successfully realized for both free running operation and active Q-switched operation through frequency doubling and sum frequency processes in a 10 mm long LBO crystal. Using the three close lasing lines of 659.5, 664 and 669 nm, it is possible to generate the multi-wavelength THz radiation of 3.42, 3.3 and 6.73 THz in an appropriate difference frequency crystal.

2. Experimental setup and results

Firstly, the simultaneous continuous wave (CW) dual-wavelength diode-end-pumped Nd:YAG laser emitting at 1319 and 1338 nm is studied. A simple linear two-mirror cavity configuration used in this experiment is shown in Fig.1.

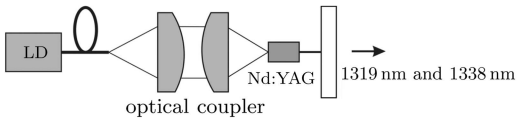


Fig.1. Experimental setup of the CW dual-wavelength laser.

The cavity length is 10 mm. A high-brightness 30 W 808 nm fibre-coupled diode laser with a fibre core diameter of 400 μm and a numerical aperture of 0.22 is employed. The multi-lens optical coupler with a 49.2 mm focal length and 90% coupling efficiency is used to re-image the pump beam onto the gain medium with a spot size of about 320 μm in diameter. The gain medium is a plano-parallel polished Nd:YAG crystal with 1.1at.-% Nd^{3+} doping level. The size of the Nd:YAG crystal is 4 mm in diameter and 6 mm in length. The pumping facet of the Nd:YAG crystal is coated with high reflectivity ($R > 99\%$) coatings at both fundamental wavelengths (1319 and 1338 nm) and second harmonic generation (SHG) wavelengths (659.5 and 669 nm), and high transmission ($T > 90\%$) coatings at 808 and 1064 nm. The output coupler is a plane mirror with partial transmission coatings at 1319 nm ($T = 10.282\%$) and 1338 nm ($T = 9.759\%$), and a high transmission ($T > 75\%$) coating at 1064 nm to suppress the oscillation at this transition. In order to obtain the high output power of the CW dual-wavelength laser, the cavity length should be as short as possible for reducing the strong thermal effect under a high pumping power condition. The temperature of the pumping source maintains 10°C by water cooling. The Nd:YAG crystal closely wrapped by a piece of indium is set in a heat sink made of the red copper and its temperature is also kept at 10°C by water cooling.

The curve for the dual-wavelength laser output power versus the pumping power is shown in Fig.2.

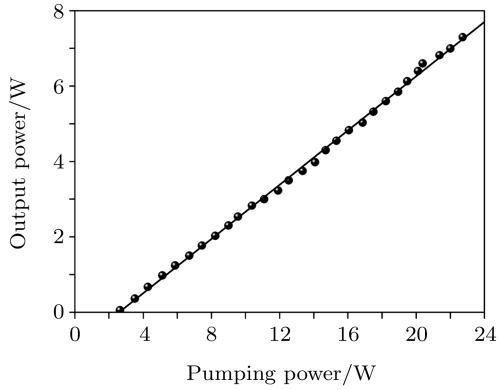


Fig.2. Output power of the dual-wavelength laser versus pumping power.

The threshold pumping power is 2.64 W, at which laser emissions at 1319 and 1338 nm simultaneously begin to oscillate. When the pumping power is increased to 22.72 W, the total output power goes up to 7.3 W with a conversion efficiency of 32.13% and a slope efficiency of 35.98%. The spectrum of the dual-wavelength laser at an output power of 6.4 W is detected by using an Agilent optical spectrum analyser (model 86142B), and the measurements are shown in Fig.3.

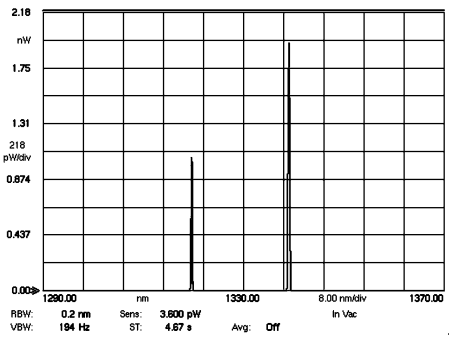


Fig.3. Spectrum of the dual-wavelength laser at an output power of 6.4 W.

We cannot exactly measure the proportion of 1319 nm or 1338 nm laser output power in a total output power due to no effective mirror separating any wavelength from the other. The line widths of 1319 nm laser and 1338 nm laser are 0.31 and 0.41 nm, respectively. The short-term instability of the output power of 6.4 W is measured and the result is shown in Fig.4. We record an output power every one minute, and in a time period of fifteen minutes, the instability of the output power can be obtained from the following formula:

$$\Delta P/\overline{P} = \sqrt{\frac{\sum_{i=1}^{n}\left(P_i-\overline{P}\right)^2}{n-1}}\cdot\frac{1}{\overline{P}} \approx 0.26\% \quad (n=15). \tag{1}$$

The measured result indicates that the output power of the CW dual-wavelength laser is very stable.

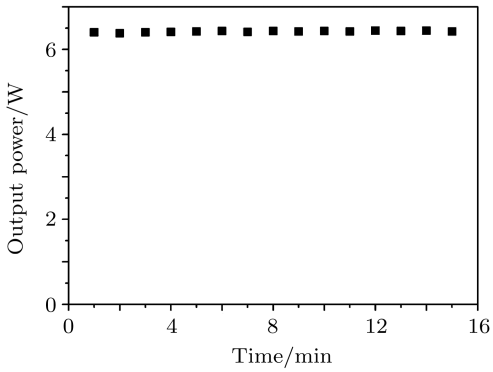


Fig.4. Short-term instability of the dual-wavelength laser output power of 6.4 W.

In order to increase the peak power of the dual-wavelength laser, we insert an acousto-optic (AO) Q-switch in the cavity. The AO Q-switch is driven at 40MHz working frequency with 7.0 W of electric power, and the modulating frequency can be continuously tuned in a range of 1–50 kHz. In our experiment, a DAST crystal is chosen to generate the difference frequency, so the linearly polarized dual-wavelength laser is needed. Inserted in the cavity is a Brewster plate, which is of a 3 mm thick quartz glass and mounted at an angle of 56° (the Brewster angle). Figure 5 shows the experimental layout of the quasi-continuous wave (QCW) linearly polarized dual-wavelength laser. The

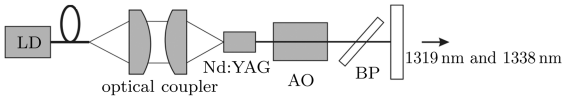


Fig.5. Experimental setup of the QCW linearly polarized dual-wavelength laser.

cavity length is 65 mm. The pumping source, the optical couplers, the Nd:YAG crystal, and the output mirror are not changed. Figure 6 shows the relation between the pumping power and the dual-wavelength laser output power at a repetition rate of 50 kHz. The

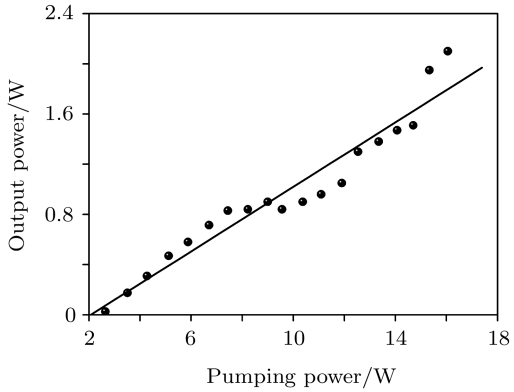


Fig.6. Output power of the dual-wavelength laser versus pumping power.

average output power is increased up to 2.1 W at a pumping power of 16.05 W, with a conversion efficiency being 13.08% and a slope efficiency being 12.86%. Figure 7 shows the spectrum of the dual-wavelength laser. The spectral line widths of 1319 nm laser and 1338 nm laser are 0.22 and 0.29 nm, respectively. The pulse width of the dual-wavelength laser with an output power of 2.1 W is 68.07ns, and the corresponding single pulse shape is shown in Fig.8. The short-term instability of the output power of 2.1 W is measured in a time period of twenty minutes, and the measured result is shown in Fig.9. The instability of the output power is less than 0.38%. The beam quality factor M^2 at the average output power of 2.1 W is measured by using the knife-edge method. The measured data and the quadratic fitting curve are shown

in Fig.10. According to the fitting coefficient and calculated equations,[24] the beam quality factor M^2 is obtained to be as low as 1.45, the width of the beam waist 69.35 μm, and the angle of divergence 0.0091rad (0.522°).

The simultaneous dual-wavelength laser provides an experimental basis for generating highly coherent and narrow linewidth THz wave radiation of 3.23 THz by using the nonlinear optical difference frequency method.

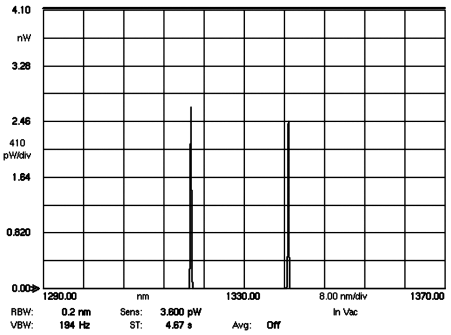


Fig.7. Spectrum of the dual-wavelength laser at an output power of 2.1 W.

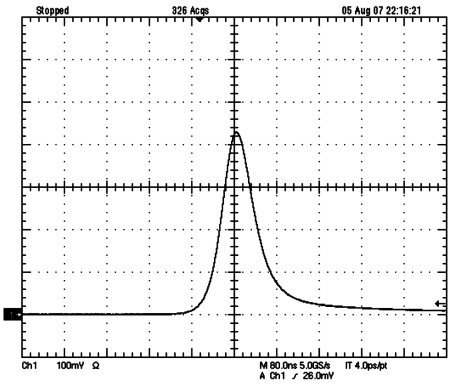


Fig.8. Single pulse shape of the dual-wavelength laser with an output power of 2.1 W.

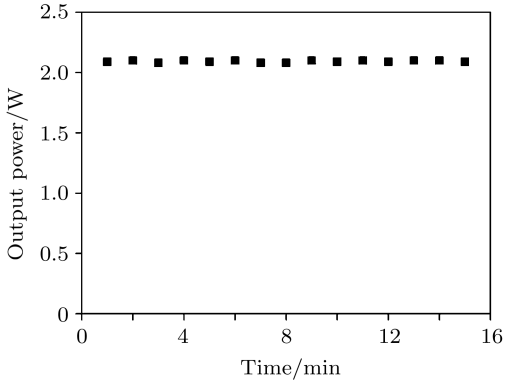


Fig.9. Short-term instability of the dual-wavelength laser output power of 2.1 W.

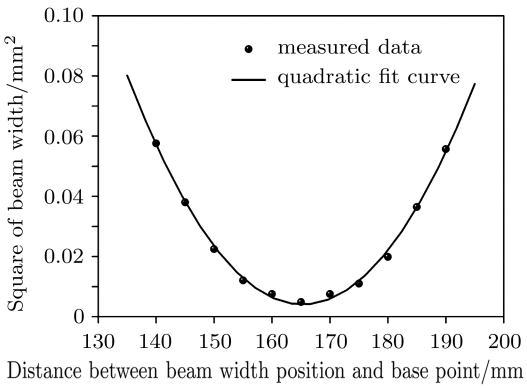


Fig.10. Distance between beam width position and base point versus square of beam width.

Not only the dual-wavelength 1319 nm/1338 nm laser but also its SHG wave can be used as a pump source of THz generator. The radiation of 659.5 nm is generated by frequency doubling of 1319 nm, and the radiation of 669 nm is generated by frequency doubling of 1338 nm. By using the dual-wavelength red laser, it is hopeful to realize the high frequency THz wave radiation of 6.73 THz. However, during our experiment, we find that the 664 nm laser which can be attributed to the sum frequency between 1319 nm and 1338 nm also exists in the red light. Because the processes of frequency doubling and sum frequency both occur, it is difficult to enhance the red-light output power and the output power stability. Using the multi-wavelength red laser, the multi-wavelength THz radiation of 6.73, 3.42 and 3.3 THz will be obtained. To the best of our knowledge, this experimental project to generate the THz wave is of great originality and it has not been reported until now.

In the reported all-solid-state intracavity frequency doubling lasers, the folded-cavity resonator is preferred to be adopted because some beam waists can be formed in the folded-cavity resonator by designing the cavity parameters appropriately, which makes it easier to improve the frequency doubling efficiency and realize the single-transverse mode laser output. However, compared with the linear-cavity resonator, the folded-cavity resonator includes more elements, thereby making the adjustment of the beam path more difficult and resulting in more losses in energy. Besides, the range of the acceptable pumping power of the folded-cavity resonator is smaller than that of the linear-cavity resonator. In our experiment, we adopt the plano-concave linear cavity to realize the stable multi-wavelength red laser operation.

Firstly, we carry out the experiment of a diode-end-pumped Nd:YAG crystal, type-I critical phase

matching LBO crystal intracavity frequency doubling CW multi-wavelength red laser. The experimental arrangement of the system is illustrated in Fig.11. We shorten the cavity length as possible as we can so as to increase the range of the permissible pumping power, and the cavity length is 21 mm. The pumping source, the optical couplers, and the Nd:YAG crystal are not changed. An LBO crystal is used as the nonlinear crystal for intracavity frequency doubling due to its high damage threshold and low absorption at both the fundamental and SHG waves of the Nd:YAG laser at 1.3 μm. The LBO crystal is cut for type-I critical phase matching of SHG ($\theta = 85.93°$, $\varphi = 0°$) and its size is $3\times3\times10\,\mathrm{mm}^3$. The phase matching angle is the mid-value between the phase matching angle of type-I critical phase matching SHG at 1319 nm($\theta = 85.85°$, $\varphi = 0°$) and that at 1338 nm($\theta = 86°$, $\varphi = 0°$). Both end faces of the LBO crystal are coated with high transmission coatings at both fundamental wavelengths (1319 and 1338 nm) and SHG wavelengths (659.5 and 669 nm). Because the permissible temperature of the LBO crystal is only 8.7 K, a temperature controller is used to maintain the temperature of the LBO crystal within an accuracy of up to ±0.1°C. The temperature of the LBO crystal is kept at 23.5°C. The output coupler is a concave mirror with a radius of curvature of 50 mm, and the mirror is coated with coatings of high transmission ($T > 95\%$) at 659.5 and 669 nm and high reflectivity ($R > 99\%$) at 1319 and 1338 nm. The output mirror is also coated with a high transmission coating at 1064 nm so as to suppress the strong parasitical oscillation at this transition.

The curve for the SHG output power versus the pumping power is shown in Fig.12. The threshold of the pumping power is 676 mW, and when the pumping power is increased to 10 W, the maximum output power of the multi-wavelength red laser of 837 mW is obtained. Figures 13(a) and 13(b) display the spectra of the red laser at the threshold and the maximum pumping powers, respectively. Two wavelengths of 659.5 and 669 nm coexist in the spectrum of the red laser at the threshold pumping power. A comparison between the intensities of the two lasing lines indicates that the 669 nm laser is nearly ignorable. The frequency component at 664 nm begins to appear with the increase of the pumping power. When the output power goes up to the maximum value, three wavelengths of 659.5, 664 and 669 nm coexist. The spectral line widths of 659.5, 664 and 669 nm lasers at a total output power of 837 mW are 0.221, 0.224 and 0.237 nm, respectively. The time trace of the red laser output power at an output power of 837 mW is shown in Fig.14. The fluctuation of the output power is better than 1.39% in a given time period of 15 minutes.

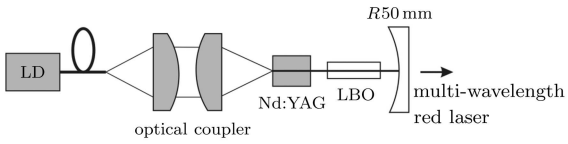


Fig.11. Experimental setup of the CW multi-wavelength red laser.

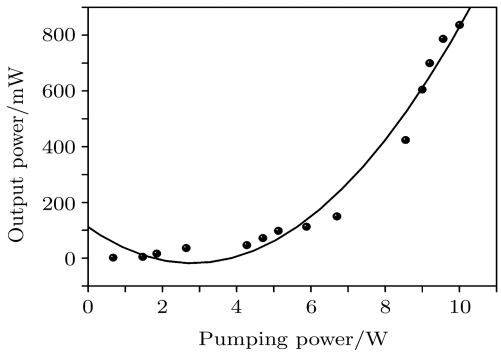


Fig.12. Output power of the CW multi-wavelength red laser versus pumping power.

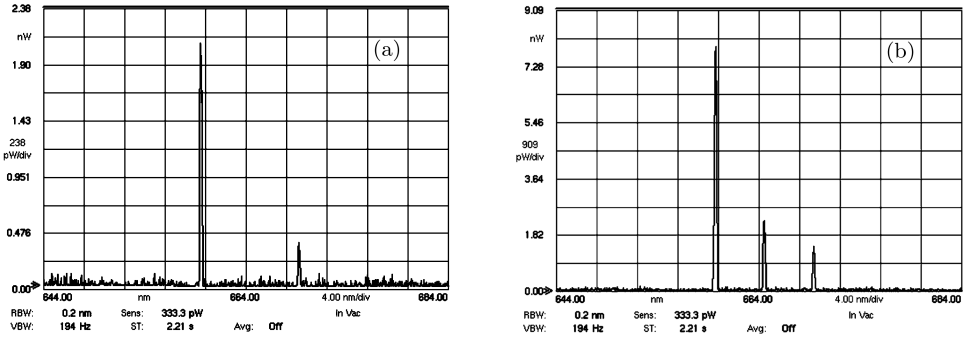


Fig.13. Spectra of the multi-wavelength red laser at the threshold pumping power (a) and at a pumping power of 10 W (b).

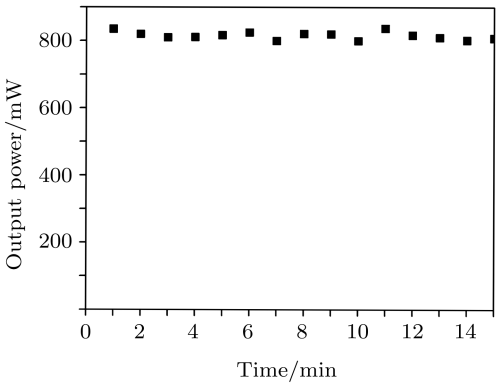


Fig.14. Short-term instability of the multi-wavelength red laser output power of 837 mW.

In order to increase the frequency doubling efficiency, we insert an AO Q-switch in the cavity to enhance the peak power of the fundamental wave, besides, set the repetition rate of the AO Q-switch to be 15 kHz. The AO Q-switch is the one which has been used in the above experiment, so its parameters are not mentioned here in detail. The schematic drawing of the experimental arrangement is indicated in Fig.15. The whole cavity resonator is very compact: the cavity length is 52 mm. The output coupler is changed for a concave mirror with a radius of curvature of 100 mm, and the coating parameters are the same as those of the above concave mirror with a radius of curvature of 50 mm. The LBO crystal is set close to the Nd:YAG crystal, because the beam waist of the fundamental wave is located on the Nd:YAG according to the cavity design, thereby achieving the strongest power density of the fundamental wave. The temperature of the LBO crystal is still set at 23.5°C.

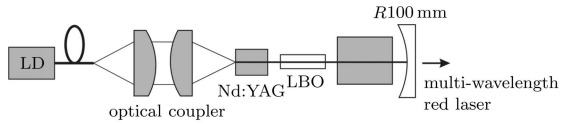


Fig.15. Experimental setup of the QCW multi-wavelength red laser.

The output power of the QCW multi-wavelength red laser at a repetition rate of 15KHz as a function of the pumping power is shown in Fig.16. The red laser output starts at a pumping power of 1.046 W when only one lasing line of 659.5 nm exists, and the red laser spectrum is shown in Fig.17(a). As pumping power increases, a second laser line at 664 nm and a third laser line at 669 nm appear sequentially. When the pumping power is increased up to 15.33 W, the average red-light output power achieves a maximum value of 1.625 W with a conversion efficiency of 10.6%, and the corresponding spectrum shown in Fig.17(b) demonstrates that there coexist three lasing lines in the red light. The output power of 659.5 nm laser still has the highest proportion of the total output power. The spectrum line widths of 659.5, 664 and 669 nm lasers at a total output power of 1.625 W are 0.202, 0.224 and 0.225 nm, respectively. The pulse width of the red laser at the output power of 1.625 W is 34.22ns,

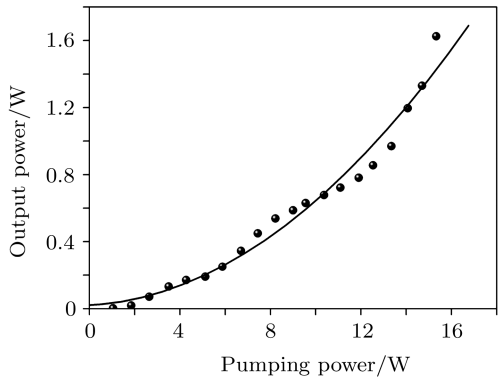
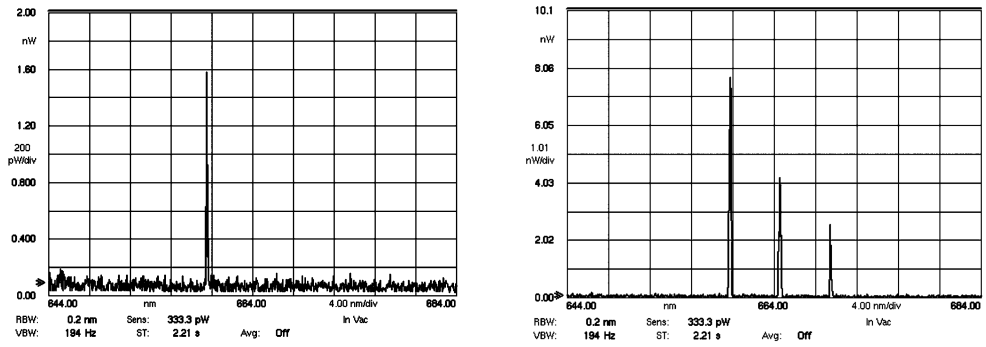


Fig.16. Output power of the QCW multi-wavelength red laser versus pumping power.



(a) (b)

Fig.17. Spectra of the multi-wavelength red laser at the threshold pumping power (a) and at a pumping power of 15.33 W (b).

and the corresponding single pulse shape is shown in Fig.18. The short-term instability of the output power of 1.625 W is measured in a time period of fifteen minutes and the measured result is shown in Fig.19. The instability of the red-light output power is less than 0.53%. The beam quality factor M^2 at the maximum output power of 1.625 W is measured by using the knife-edge method. Figure 20 shows the measured data and the quadratic fitting curve. The beam quality factor M^2 is 6.05, the width of the beam waist is 98.35 μm, and the angle of divergence is 0.013rad (0.746°). The measured result indicates that the beam quality of the multi-wavelength red laser is not very satisfactory, because the simple plano-concave linear cavity resonator is used to generate the red laser. If we adopt a folded-cavity resonator to generate the red laser in the future, the beam quality of the red laser should be improved.

The diode-end-pumped Nd:YAG LBO intracavity frequency doubling multi-wavelength CW and QCW red-light stable outputs are both realized successfully. Using the three lasing lines, the multi-wavelength THz radiation of 6.73, 3.42, and 3.3 THz can be generated by using the optical difference frequency technology.

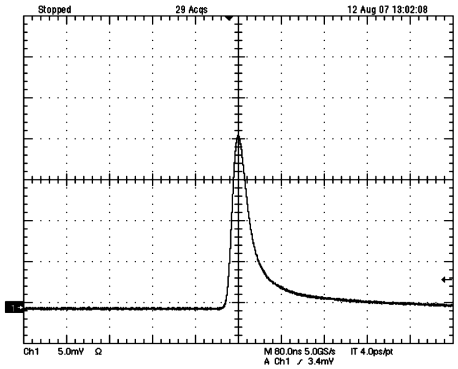


Fig.18. Single pulse shape of the multi-wavelength red laser with an output power of 1.625 W.

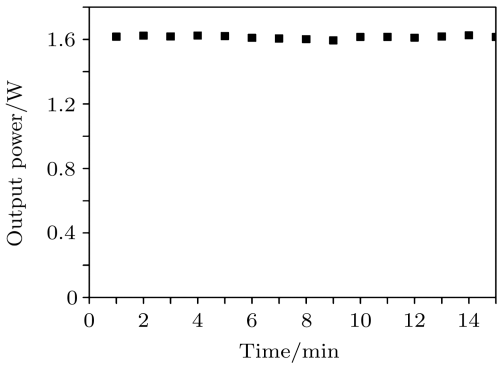


Fig.19. Short-term instability of the multi-wavelength red laser output power of 1.625 W.

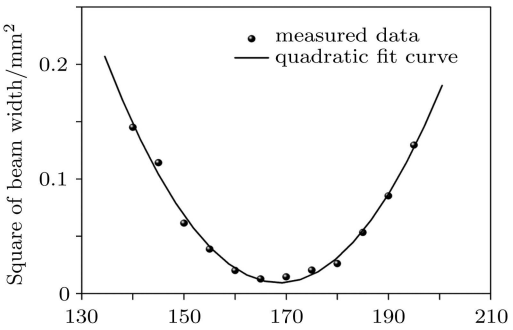


Fig.20. Distance between beam width position and base point versus square of beam width.

3. Conclusion

The diode-end-pumped Nd:YAG 1319 nm/1338 nm CW and QCW dual-wavelength lasers and the diode-end-pumped Nd:YAG LBO intracavity frequency doubling CW and QCW multi-wavelength red lasers are demonstrated. The output power of the CW dual-wavelength laser is enhanced up to 7.3 W at a pumping power of 22.72 W. The power fluctuation is less than 0.26% at the output power of 6.4 W. The QCW linearly polarized dual-wavelength laser maximum average output power is achieved to be 2.1 W at a repetition rate of 50 kHz and a pumping power of 16.05 W, and the corresponding pulse width is 68.07ns. At the output power of 2.1 W, the short-term power instability is less than 0.38% and the beam quality factor M^2 is as low as 1.45. Using the simultaneous two lines, the highly coherent THz wave radiation of 3.23 THz can be generated in a 1 mm thick DAST crystal by using the nonlinear optical difference frequency method.

Based on the stable output of the fundamental dual-wavelength laser, the multi-wavelength red laser is generated through intracavity frequency doubling and sum frequency in an LBO crystal. The maximum output power of the CW multi-wavelength red laser is 837 mW at a pumping power of 10 W, when the instability of the output power is better than 1.39% in a given time period of 15 minutes. The average output power of the QCW multi-wavelength red laser increases up to 1.625 W at a repetition rate of 15 kHz and a pumping power of 15.33 W, when the pulse width is 34.22ns, the instability of the output power is less than 0.53% and the beam quality factor M^2 is 6.05. Simultaneous dual-wavelength and multi-wavelength lasers will carve out a new way for developing all-solid-state, room-temperature running, well-compactness, and coherent tabletop THz radiation sources.

References

[1] Siegel P H 2002 *IEEE Trans. Microwave Theory and Tech.* **50** 910

[2] Köhler R, Tredicucci A, Beltram F, Beere H E, Linfield E H, Davies A G, Ritchie D A, Iotti R C and Rossi F 2002 *Nature* **417** 156

[3] Sherwin M 2002 *Nature* **420** 131

[4] Weiss C, Torosyan G, Avetisyan Y and Beigang R 2001 *Opt. Lett.* **26** 563

[5] Wu L, Zhang X C and Auston D H 1992 *Appl. Phys. Lett.* **61** 1784

[6] Zernike F and Berman Jr P R 1965 *Phys. Rev. Lett.* **15** 999

[7] Yajima T and Inoue K 1969 *IEEE J. Quantum Electron.* **QE-5** 140

[8] Kawase K, Mizuno M, Sohma S, Takahashi H, Taniuchi T, Urata Y, Wada S, Tashiro H and Ito H 1999 *Opt. Lett.* **24** 1065

[9] Kawase K, Hatanaka T, Takahashi H, Nakamura K, Taniuchi T and Ito H 2000 *Opt. Lett.* **25** 1714

[10] Shi W, Ding Y J, Fernelius N and Vodopyanov K 2002 *Opt. Lett.* **27** 1454

[11] Tanabe T, Suto K, Nishizawa J, Saito K and Kimura T 2003 *J. Appl. Phys.* **93** 4610

[12] Taniuchi T, Adachi H, Okada S, Sasaki T and Nakanishi H 2004 *Electron. Lett.* **40** 549

[13] Suizu K, Miyamoto K, Yamashita T and Ito H 2007 *Opt. Lett.* **32** 2885

[14] Shi W and Ding Y J 2005 *Opt. Lett.* **30** 1030

[15] Ding Y J and Shi W 2006 *Laser Phys.* **16** 562

[16] Shen H Y and Su H 1999 *J. Appl. Phys.* **86** 6647

[17] Shen H Y, Lin W X, Zeng R R, Zhou Y P, Yu G F, Huang C H, Zeng Z D, Zhang W L, Wu R F and Ye Q L 1993 *Appl. Opt.* **32** 5952

[18] Wang C Q, Chow Y T, Yuan D R, Xu D, Zhang G H, Liu M G, Lu J R, Shao Z S and Jiang M H 1999 *Opt. Commun.* **165** 231

[19] Lin W X and Shen H Y 1999 *Acta Phys. Sin.* **48** 667 (in Chinese)

[20] Chen Y F 2000 *Appl. Phys. B* **70** 475

[21] Li P X, Li D H, Li C Y and Zhang Z G 2004 *Chin. Phys.* **13** 1689

[22] Zhang Q, Yao J Q, Wen W Q, Liu H, Ding X and Zhou R 2006 *Chin. Journal of Lasers* **33** 577 (in Chinese)

[23] Ardhendu S, Aniruddha R, Sourabh M, Nandita S, Prasanta K D and Pranab K D 2006 *Opt. Express* **14** 4721

[24] Lü B D 2003 *Laser Optics—Beam Characterization, Propagation and Transformation, Resonator Technology and Physics* (Beijing: Higher Education Press) p83